Supporting Information for "AMOC Stabilization under the Interaction with Tipping Polar Ice Sheets"

S. Sinet[1,2], A. S. von Der Heydt[1,2], and H. A. Dijkstra[1,2]

[1]Department of Physics, Institute for Marine and Atmospheric Research Utrecht, Utrecht University, Utrecht, The Netherlands

[2]Center for Complex Systems Studies, Department of Physics, Utrecht University, Utrecht, The Netherlands

Contents of this file

Introduction

In this document, we provide a more detailed description of the Greenland Ice Sheet (GIS), Atlantic Meridional Overturning Circulation (AMOC) and West Antarctica Ice Sheet (WAIS) models through texts S1 to S3, and describe the construction of the initial state in the text S4. Finally, we describe our numerical resolution in section S5.

S1. The GIS model

We consider an isothermal ice sheet lying on a fixed bedrock (Greve & Blatter, 2009). The evolution of the ice thickness h is given by the contribution of the transport inside the ice dome involving the ice flux F, along with the Surface Mass Balance (SMB) a (positive or negative in case of respectively freezing or melting), condensed in the continuity equation

$$\frac{\partial h}{\partial t} = -\nabla \cdot F + a. \tag{1}$$

In the case of an isothermal ice sheet, the problem is simplified by using the Shallow Ice Approximation (SIA) giving an expression for the flux. To simplify the problem further, we consider a radially symmetric ice cap resting on a flat circular bed of radius R at sea level. Also, the SMB will be expressed as a function of the ice elevation alone such that, in polar coordinates, the system of equations is

$$\frac{\partial h}{\partial t} = -\frac{1}{r}\frac{\partial}{\partial r}(rF) + a(h) \tag{2}$$

$$F = -A_0 \frac{\partial h}{\partial r}\left|\frac{\partial h}{\partial r}\right|^{n-1} h^{n+2}, \tag{3}$$

to which we add the no-ice condition $h = 0$ for $r \geq L(t)$, where we denote by $L(t)$ the radial position of the ice margin, such that $L(t) \leq R$ at all time. Also,

$$A_0 = \frac{2A(\rho_i g)^n}{n+2}, \tag{4}$$

where A is the ice viscosity parameter, ρ_i the ice density, g the gravitational acceleration and n the exponent used in the Glenn's flow law. This system describes a free boundary problem (Schoof & Hewitt, 2013) and, in this case of purely height-dependant SMB, the domain at steady state will necessarily be totally ice-covered or ice-free. Solving this

equation numerically is subtle, and our approach is presented in the text S5.1. Following (Greve & Blatter, 2009), we represent the height-SMB feedback by expressing a in a simple form, involving only three parameters

$$a(h) = \min\left[P, m\left(h - h_{el}\right)\right], \tag{5}$$

namely the melting gradient m, the precipitation rate P and the equilibrium line altitude h_{el}. The latter two are made temperature dependant by assuming that their present-day (inter glacial) and glacial climate values are linearly related with respect to the temperature anomaly in the northern hemisphere $\Delta\tau_N$. It means

$$P(\Delta\tau_{\mathrm{N}}) = P_{IG} + \frac{P_G - P_{IG}}{\Delta\tau_{N,G}}\Delta\tau_{\mathrm{N}},$$
$$h_{el}(\Delta\tau_{\mathrm{N}}) = h_{el,IG} + \frac{h_{el,\mathrm{G}} - h_{el,IG}}{\Delta\tau_{N,G}}\Delta\tau_{\mathrm{N}},$$

where indexes G and IG stand for respectively the glacial and inter glacial climates. All parameter values are presented in table S1.

To compute the meltwater flux F_N, we express mass conservation by integrating the continuity equation 2 over the whole domain. Performing the integration and using the Leibniz integral rule for the l.h.s. we get, considering that $h(L(t)) = 0$ by definition,

$$\frac{\partial V}{\partial t} = -2\pi L(t)F(L(t)) + 2\pi\int_0^{L(t)} a(h)r dr. \tag{6}$$

The SMB can be separated into a precipitation component P and a melting component M. Consistently with equation 5, P is constant over the domain such that we can write

$$\frac{\partial V}{\partial t} = \pi L^2(t)P - 2\pi L(t)F(L(t)) + 2\pi\int_0^{L(t)} M(h)r dr. \tag{7}$$

In the r.h.s, the outflux is represented by calving (second term) and melting (third term). Hence, we define the meltwater flux positively as

$$F_N = \frac{\rho_i}{\rho_w}\left(\pi L^2(t)P - \frac{\partial V}{\partial t}\right), \tag{8}$$

where the prefactor ρ_i/ρ_w stands for the conversion of the ice volume into a water volume.

S2. The AMOC model

We use the model of Rooth (Rooth, 1982) as presented in (Lucarini & Stone, 2005), where the AMOC is depicted by 3 boxes yielding a thermohaline circulation driven by the pole-to-pole density difference. Respectively, the first box represents the northern Atlantic Ocean above 30°N, the second box represents the tropical region between 30°N and 30°S, and the third box represents the southern Atlantic Ocean under 30°S. Hence, to some approximation, the equatorial box is two times the volume of each polar boxes, defining the box volume ratio $V = V_2/V_1 = V_2/V_3 = 2$. From the temperature T_j and salinity S_j of one box, the density ρ_j for $j = \{1, 2, 3\}$ is approximated by

$$\rho_j(T_j, S_j) \approx \rho_w(1 - \alpha T_j + \beta S_j), \tag{9}$$

where ρ_w is the reference water density, α is the thermal expansion coefficient and β the haline expansion coefficient. The AMOC strength q is then directly computed using the normalised pole-to-pole density difference

$$q = \frac{k}{\rho_w}(\rho_1 - \rho_3) \tag{10}$$

$$= k\left[\alpha\left(T_3 - T_1\right) + \beta\left(S_1 - S_3\right)\right], \tag{11}$$

with k the hydraulic constant, used for fitting q to a reasonable value. Considering a circulation with northern sinking ($q > 0$), the dynamical equations are given by the

variation of temperatures and salinities

$$\frac{\partial T_1}{\partial t} = q\,(T_2 - T_1) + \lambda(\tau_1 - T_1), \tag{12}$$
$$\frac{\partial T_2}{\partial t} = \frac{q}{V}\,(T_3 - T_2) + \lambda(\tau_2 - T_2), \tag{13}$$
$$\frac{\partial T_3}{\partial t} = q\,(T_1 - T_3) + \lambda(\tau_3 - T_3), \tag{14}$$
$$\frac{\partial S_1}{\partial t} = q\,(S_2 - S_1) - (\bar{F}_1 + \bar{F}_N), \tag{15}$$
$$\frac{\partial S_2}{\partial t} = \frac{q}{V}\,(S_3 - S_2) + \frac{(\bar{F}_1 + \bar{F}_N + \bar{F}_3 + \bar{F}_S)}{V}, \tag{16}$$
$$\frac{\partial S_3}{\partial t} = q\,(S_1 - S_3) - (\bar{F}_3 + \bar{F}_S). \tag{17}$$

All the parameters involved are presented in table S1. Both temperatures and salinities are transported via an advection term implying the AMOC strength q. The temperature of each box is relaxed to a target temperatures τ_i, at a timescale given by the relaxation constant λ (corresponding to about 25 yr). Salinities are forced by freshwater fluxes including precipitation $F_{1,3}$ and meltwater fluxes $F_{N,S}$ in the poles, compensated by evaporation in the tropics. In the equations, those are expressed by virtual salinity fluxes $\bar{F}_i$ through scaling, i.e. for $i \in \{1, N, 3, S\}$,

$$\bar{F}_i = \frac{S_0 \rho_w}{M} F_i, \tag{18}$$

where M is the mass of polar boxes and S_0 the average salinity. Note that the evaporation term in equation 16 imposes average salinity conservation. Finally, this model applied to a southern sinking configuration implies a permutation of temperatures and salinites in the r.h.s. of each equation (Scott et al., 1999). The system is not differentiable at this transition - we show in the text S5.2 how to handle it in our numerical resolution.

S3. The WAIS model

The WAIS, here considered as one single Marine Ice Sheet (MIS), is represented using a depth integrated Shallow Shelf Approximation (SSA) as in (Schoof, 2007). In the case of a rapidly sliding, two-dimensional and symmetrical MIS, the dynamical equations are given by

$$\frac{\partial h}{\partial t} + \frac{\partial (uh)}{\partial x} = a, \tag{19}$$

$$\frac{\partial}{\partial x}\left[2\bar{A}^{-1/n} h \left|\frac{\partial u}{\partial x}\right|^{(1/n)-1} \frac{\partial u}{\partial x}\right] - C|u|^{(m-1)}u - \rho_i g h \frac{\partial (h-b)}{\partial x} = 0. \tag{20}$$

Here, b is the depth of the bedrock (positive when under sea level), u is the depth integrated flow inside the bulk, $\bar{A}$ is the depth integrated viscosity parameter, while C and m define the sliding law. Note that we consider the accumulation a constant in time and over the whole domain. The ice shelve is included as a border condition at the grounding line, i.e. at $x = x_g$,

$$2\bar{A}^{-1/n} \left|\frac{\partial u}{\partial x}\right|^{(1/n)-1} \frac{\partial u}{\partial x} = \frac{1}{2}\left(1 - \frac{\rho_i}{\rho_w}\right)\rho_i g h, \tag{21}$$

to which we add the flotation requirement

$$\rho_i h = \rho_w b. \tag{22}$$

Finally, at $x = 0$, we add the symmetry requirement

$$\frac{\partial (h-b)}{\partial x} = 0. \tag{23}$$

All the parameters involved are defined in table S1. It is important to note that, in what follows, we extend this model to one supplementary horizontal dimension of length y_0 with respect to which the MIS yields translational symmetry.

To compute the hosing flux F_S, we express mass conservation by integrating the continuity equation 19 over the whole domain. Performing the integration and using the Leibniz integral rule for the l.h.s. we get

$$\frac{\partial V}{\partial t} - 2y_0 h(x_g(t)) \frac{\partial x_g(t)}{\partial t} = -2y_0 h(x_g(t)) u(x_g(t)) + 2y_0 \int_0^{x_g(t)} a dx. \tag{24}$$

Here, we consider no surface melting, such that the SMB only contains a constant and homogeneous precipitation rate P. Hence we write

$$\frac{\partial V}{\partial t} = 2y_0 x_g(t) P - 2y_0 h(x_g(t)) \left(u(x_g(t)) - \frac{\partial x_g(t)}{\partial t} \right). \tag{25}$$

The only contribution to outflux is the ice flux through the moving grounding line, analogous to a calving process (Benn et al., 2007). Hence, assuming the ice outflux to instantaneously transform into meltwater, we get the meltwater outflux

$$F_S = 2 \frac{\rho_i}{\rho_w} y_0 h(x_g(t)) \left(u(x_g(t)) - \frac{\partial x_g(t)}{\partial t} \right) f, \tag{26}$$

where the prefactor ρ_i / ρ_w stands for the conversion of the ice volume into a water volume. Also, to consider loss of freshwater into the Pacific Ocean, we add a parameter f fixing the fraction of the total meltwater outflux entering the South Atlantic Ocean. To estimate f, we consider the definition of the WAIS drainage basins of Rignot et al. (2019) used in the Ice sheet Mass Balance Inter-comparison Exercise (IMBIE), and assume only the basins draining into the Ronne ice shelf to contribute to the hosing of the southern Atlantic Ocean. Hence, we approximate f by computing the mass ratio between the Ronne draining basin and the entire WAIS, using present-day values (Morlighem et al., 2020).

S4. Construction of the initial state

At initial state, we want the AMOC to be in a northern sinking configuration similar to present-day. To fix it, we set the total freshwater flux in the polar boxes to the values used in (Lucarini & Stone, 2005). In term of virtual salinity fluxes, we have at initial state (denoted by the exponent 0)

$$\bar{F}_1^0 + \bar{F}_N^0 = 13.50 \cdot 10^{-11} \text{ psu s}^{-1}, \tag{27}$$

$$\bar{F}_3^0 + \bar{F}_S^0 = 9.00 \cdot 10^{-11} \text{ psu s}^{-1}, \tag{28}$$

where $\bar{F}_{S,N}^0$ are given once the initial state of ice caps is fixed. On one hand, the only free parameter to tune for the GIS is the radius of the bedrock R. On the other hand, the WAIS model still contains two free parameters, namely $\bar{A}^0$ and y_0, the first being the depth integrated viscosity parameter at initial state. Those are tuned to fit both ice sheet volumes to present-day values (Morlighem et al., 2017, 2020). Those parameters and relevant quantities are summarised in table S2.

We note that the (total) outflux at initial state is slightly overestimated for both ice sheets when compared to present-day estimations (The IMBIE Team, 2018, 2020), due the the limited degrees of freedom. We prioritized the fit to the volume estimations from the literature as this is the quantity that will ultimately dictate the stabilizing and destabilizing effects. Indeed, meltwater fluxes at initial state are absorbed by the values of $\bar{F}_{1,3}^0$ via equation 27 and 28. Finally, we note that the AMOC strength of the hence constructed initial state is in agreement with the values from the RAPID-AMOC programme (McCarthy et al., 2015).

S5. Numerical resolution

The full model is solved with implicit time stepping, using a monolithic approach. The state vector X is given at any time by

$$X(t) = \begin{bmatrix} x_{\mathrm{WAIS}}(t) \\ x_{\mathrm{AMOC}}(t) \\ x_{\mathrm{GIS}}(t) \end{bmatrix}, \tag{29}$$

such that the whole system can be expressed as

$$B\dot{X}(t) = F(X(t), \mu), \tag{30}$$

with μ some (possibly time dependant) parameters, and B a linear operator. From there, we perform the time integration using a θ-method

$$B\frac{X\left(t_{k+1}\right) - X\left(t_k\right)}{\Delta t} = (1-\theta)F\left(X\left(t_k\right), \mu\right) + \theta F\left(X\left(t_{k+1}\right), \mu\right), \quad \theta \in [0,1]., \tag{31}$$

choosing $\theta = 0.7$. As this equation is generally highly non-linear, solving it requires using a root finding algorithm. We use a Newton iteration, involving the Jacobian of the full system

$$J_{ij}(X) = \frac{\partial F_i(X)}{\partial X_j}, \tag{32}$$

which has the following structure

$$J = \begin{pmatrix} J_{\mathrm{WAIS}} & J_{\mathrm{AMOC}\to\mathrm{WAIS}} & 0 \\ J_{\mathrm{WAIS}\to\mathrm{AMOC}} & J_{\mathrm{AMOC}} & J_{\mathrm{GIS}\to\mathrm{AMOC}} \\ 0 & 0 & J_{\mathrm{GIS}} \end{pmatrix}, \tag{33}$$

Where $J_{\mathrm{WAIS}\to\mathrm{AMOC}}$ and $J_{\mathrm{GIS}\to\mathrm{AMOC}}$ contain the coupling via meltwater fluxes from the ice sheets to the AMOC, while $J_{\mathrm{AMOC}\to\mathrm{WAIS}}$ contains the coupling from the southern Atlantic Ocean temperature to the WAIS via the depth integrated ice viscosity parameter $\bar{A}$. This sparse structure allows to divide the resolution of the Jacobian when performing Newton iterations.

S5.1. The GIS model

Given the radial symmetry, the domain is a straight line of constant length R. We use a staggered grid made of $N = 750$ main points numbered $i = 1, \cdots, N$, and a secondary grid falling in between the main grid points, numbered by half integers $i \pm \frac{1}{2}$. The discretization has been chosen such that the axis of symmetry of the ice cap corresponds to the point $1 - \frac{1}{2}$ while the margin falls at $N + 1$.

The effective diffusivity D is defined on the secondary grid for $i = 1, \cdots, N$ by

$$D_{i+\frac{1}{2}} = \frac{A_0}{2}(r_i + r_{i+1}) \left(\frac{h_i + h_{i+1}}{2} \right)^5 \left(\frac{h_{i+1} - h_i}{\Delta r} \right)^2, \tag{34}$$

so that the flux is given by

$$F_{i+\frac{1}{2}} = -\frac{1}{\Delta r} D_{i+\frac{1}{2}} (h_{i+1} - h_i). \tag{35}$$

While the diffusivity term is not defined at $i = 1 - \frac{1}{2}$, the symmetry of the problem directly gives us the border condition for the flux at the axis of symmetry, $F_{1-\frac{1}{2}} = 0$. The dynamical equation then relates the ice elevation at time n and $n + 1$ in a fully implicit scheme

$$\frac{h_i^{n+1} - h_i^n}{\Delta t} = -\frac{1}{r_i^{n+1} \Delta r} \left(F_{i+\frac{1}{2}}^{n+1} - F_{i-\frac{1}{2}}^{n+1} \right) + a_i^{n+1}. \tag{36}$$

As the implicitness requires differentiability, we truncate the SMB a by smoothening the min function using the primitive of the logistic function, also known as the softplus function, widely used in neural networks, see for example (Glorot et al., 2011). In our case, it takes the form

$$a(h) = m \left[h - \frac{P}{m} - h_{el} - \frac{1}{k} \log \left(e^{k\left(h - \frac{P}{m} - h_{el}\right)} + 1 \right) \right] + P, \tag{37}$$

where it is understood that $P = P(\Delta\tau_N)$ and $h_{el} = h_{el}(\Delta\tau_N)$. k is a convergence parameter which we set to 300.

Note that, during the resolution, all the points of the domain are treated equally, meaning that the ice thickness naturally gets negative on the border and where the is no more ice. Hence, at each time step, all negative thicknesses are set to 0. While this yields significant errors in the position and thickness gradient at the margin, it has been shown to have only little effect on the global behaviour of the ice sheet in the isothermal case, as long as the resolution is high enough (Bueler et al., 2005; Van Den Berg et al., 2006).

In the coupled model, we also need to express margin position $L(t)$ and volume of the ice cap V to compute the meltwater outflux. As each time step potentially involves negative ice thicknesses, those quantities involve integrals on the ice covered domain only, hence on the domain $[0\ L(t)]$. However, they can be defined by integrating on the whole domain $[0\ R]$ using a theta function. Respectively,

$$L(t) = \int_0^{L(t)} \mathrm{d}r \tag{38}$$

$$= \int_0^R \Theta\left[h(r)\right] \mathrm{d}r, \tag{39}$$

and

$$V = \pi \int_0^L h(r) \cdot \mathrm{d}(r^2) \tag{40}$$

$$= \pi \int_0^R h(r) \cdot \Theta\left[h(r)\right] \mathrm{d}(r^2), \tag{41}$$

in which the theta function is approximated by a logistic function while the integral is computed by trapezoidal rule.

S5.2. The AMOC model

When the circulation changes direction, the advection term undergoes some permutations (Scott et al., 1999). To use implicit time stepping, we need to smoothen this transition. In line with (Titz et al., 2002), we define q_+ and q_- as

$$q_+ = \frac{q}{1 - e^{-kq}}, \tag{42}$$

$$q_- = \frac{q}{1 - e^{kq}}, \tag{43}$$

with k the fitting parameter, a non physical constant here set to 200. We can then replace the advection term using those two contributions. For example, equation 12 becomes

$$\dot{T}_1 = q_+ (T_2 - T_1) + q_- (T_1 - T_3) + \lambda(\tau_1 - T_1). \tag{44}$$

S5.3. The WAIS model

Our numerical scheme follows the approach in (Mulder et al., 2018) without change.

References

Benn, D. I., Hulton, N. R., & Mottram, R. H. (2007). 'calving laws', 'sliding laws' and the stability of tidewater glaciers. *Annals of Glaciology*, *46*, 123–130. doi: 10.3189/172756407782871161

Bueler, E., Lingle, C. S., Kallen-Brown, J. A., Covey, D. N., & Bowman, L. N. (2005). Exact solutions and verification of numerical models for isothermal ice sheets. *Journal of Glaciology*, *51*(173), 291–306. doi: 10.3189/172756505781829449

Glorot, X., Bordes, A., & Bengio, Y. (2011). Deep sparse rectifier neural networks. In *Proceedings of the fourteenth international conference on artificial intelligence and statistics* (Vol. 15, pp. 315–323). Fort Lauderdale, FL, USA: Proceedings of Machine

Learning Research.

Greve, R., & Blatter, H. (2009). *Dynamics of ice sheets and glaciers*. Berlin, Germany: Springer.

Lucarini, V., & Stone, P. H. (2005). Thermohaline circulation stability: a box model study. Part I: uncoupled model. *Journal of Climate*, *18*(4), 501 - 513. doi: 10.1175/JCLI-3278.1

McCarthy, G. D., Smeed, D. A., Johns, W. E., Frajka-Williams, E., Moat, B. I., Rayner, D., ... Bryden, H. L. (2015). Measuring the Atlantic Meridional Overturning Circulation at 26°N. *Progress in Oceanography*, *103*, 91–111.

Morlighem, M., Rignot, E., Binder, T., Blankenship, D., Drews, R., Eagles, G., ... Young, D. (2020). Deep glacial troughs and stabilizing ridges unveiled beneath the margins of the Antarctic ice sheet. *Nature Geoscience*, *13*, 1-6. doi: 10.1038/s41561-019-0510-8

Morlighem, M., Williams, C. N., Rignot, E., An, L., Arndt, J. E., Bamber, J. L., ... Zinglersen, K. B. (2017). BedMachine v3: Complete bed topography and ocean bathymetry mapping of Greenland from multibeam echo sounding combined with mass conservation. *Geophysical Research Letters*, *44*(21), 11,051-11,061. doi: https://doi.org/10.1002/2017GL074954

Mulder, T. E., Baars, S., Wubs, F. W., & Dijkstra, H. A. (2018). Stochastic marine ice sheet variability. *Journal of Fluid Mechanics*, *843*, 748–777. doi: 10.1017/jfm.2018.148

Rignot, E., Mouginot, J., Scheuchl, B., van den Broeke, M. R., van Wessem, M., &

Morlighem, M. (2019). Four decades of Antarctic Ice Sheet mass balance from 1979–2017. *Proceedings of the National Academy of Sciences of the United States of America*, *116*, 1095 - 1103.

Rooth, C. (1982). Hydrology and ocean circulation. *Progress in Oceanography*, *11*(2), 131-149. doi: https://doi.org/10.1016/0079-6611(82)90006-4

Schoof, C. (2007). Ice sheet grounding line dynamics: Steady states, stability, and hysteresis. *Journal of Geophysical Research*, *112*, F03S28. doi: 10.1029/2006JF000664

Schoof, C., & Hewitt, I. (2013). Ice-sheet dynamics. *Annual Review of Fluid Mechanics*, *45*(1), 217-239. doi: 10.1146/annurev-fluid-011212-140632

Scott, J. R., Marotzke, J., & Stone, P. H. (1999). Interhemispheric thermohaline circulation in a coupled box model. *Journal of Physical Oceanography*, *29*(3), 351 - 365. doi: 10.1175/1520-0485(1999)029⟨0351:ITCIAC⟩2.0.CO;2

The IMBIE Team. (2018). Mass balance of the Antarctic Ice Sheet from 1992 to 2017. *Nature*, *558*, 219-222. doi: 10.1038/s41586-018-0179-y

The IMBIE Team. (2020). Mass balance of the Greenland Ice Sheet from 1992 to 2018. *Nature*, *579*, 233–239. doi: 10.1038/s41586-019-1855-2

Titz, S., Kuhlbrodt, T., Rahmstorf, S., & Feudel, U. (2002). On freshwater-dependent bifurcations in box models of the interhemispheric thermohaline circulation. *Tellus A: Dynamic Meteorology and Oceanography*, *54*(1), 89-98. doi: 10.3402/tellusa.v54i1.12126

Van Den Berg, J., Van De Wal, R., & Oerlemans, J. (2006). Effects of spatial discretization in ice-sheet modelling using the shallow-ice approximation. *Journal of*

Glaciology, *52*(176), 89–98. doi: 10.3189/172756506781828935

Table S1. Parameters involved each model.

Model	Quantity	Symbol	Value
	Gravitational acceleration	g	$9.81 \cdot 10^6$ m s^{-2}
	Ice density	ρ_I	910 kg m^{-3}
	(Reference) water density	ρ_w	1000 kg m^{-3}
	Glenn exponent	n	3
GIS	Ice viscosity parameter	A	$3.17 \cdot 10^{-24}$ Pa^{-3} s^{-1}
	Melting gradient	m	0.005 years^{-1}
	Present-day temperature anomaly	$\Delta\tau_{N,IG}$	0 °C
	Present-day Snowfall rate	P_{IG}	0.3 m years^{-1}
	Present-day equilibrium line altitude	$h_{el,IG}$	1100 m
	Glacial temperature anomaly	$\Delta\tau_{N,G}$	-10 °C
	Glacial Snowfall rate	P_G	0.15 m years^{-1}
	Glacial equilibrium line altitude	$h_{el,G}$	100 m
AMOC	Mass of the polar boxes	M	$1.08 \cdot 10^{20}$ kg
	Box volume ratio	V	2
	Average salinity	S_0	35 psu
	Thermal expansion coefficient	α	$1.5 \cdot 10^{-4}$ °C^{-1}
	Haline expansion coefficient	β	$8 \cdot 10^{-4}$ psu^{-1}
	Hydraulic constant	k	$1.5 \cdot 10^{-6}$ s^{-1}
	Target temperature (box 1)	τ_1	0 °C
	Target temperature (box 2)	τ_2	30 °C
	Target temperature (box 3)	τ_3	0 °C
	Newtonian relaxation constant	λ	$1.29 \cdot 10^{-9}$ s^{-1}
WAIS	Surface mass balance	a	0.3 m years^{-1}
	Frictional constant	C	$7.62 \cdot 10^6$ Pa m$^{-\frac{1}{3}}$ s$^{\frac{1}{3}}$
	Sliding law exponent	m	1/3

Table S2. Relevant quantities defining the initial state. Quantities marked with an asterisk are tuned degrees of freedom.

Model	Quantity	Symbol	Initial state
GIS	Bedrock radius*	R	682 km
	Volume	V_N^0	$2.99 \cdot 10^6$ km^3
	Total meltwater flux	F_N^0	$1.27 \cdot 10^{-2}$ Sv
AMOC	Strength	q^0	15.9 Sv
	Precipitation in box 1	F_1^0	0.40 Sv
	Precipitation in box 3	F_3^0	0.28 Sv
WAIS	Fraction parameter	f	0.27
	Zonal extension*	y_0	358 km
	Depth integrated viscosity parameter*	$\bar{A}^0$	$2 \cdot 10^{-25}$ Pa^{-3}s^{-1}
	Volume	V_S^0	$3.39 \cdot 10^6$ km^3
	Total meltwater flux	F_S^0/f	$0.85 \cdot 10^{-2}$ Sv

Figure S1. Range over which the critical value of global warming leading to AMOC tipping $\Delta\tau_{G,c}$ varies as the coupling c_s ranges from 0 to 1, depending on the fraction f of the outflux from WAIS reaching the Southern Atlantic Ocean. The vertical line lies at our estimation $f = 0.27$.

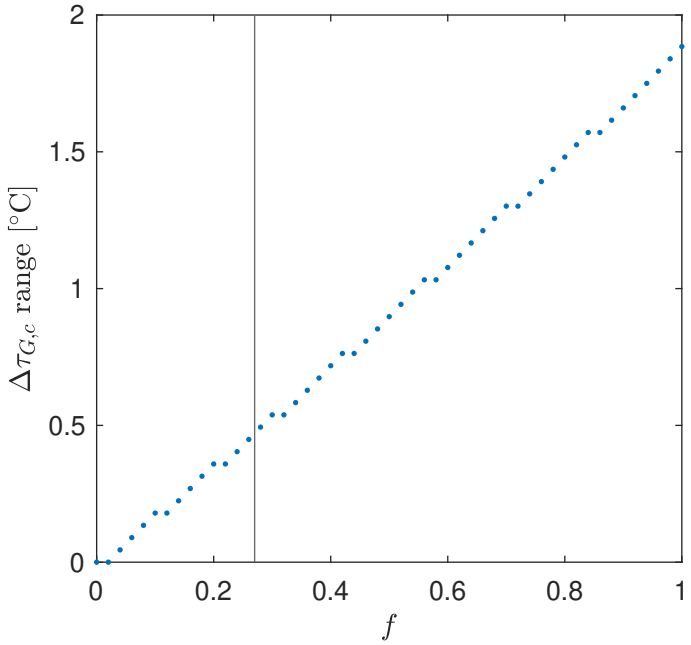

Figure S2. Transient behavior of the coupled model in hosing experiments. We represent GIS and WAIS meltwater fluxes in regimes where the AMOC does not tip (a,c) or tips (b,d). Each graph corresponds to different values of the parameter vector $(c_S, \Delta t)$: (a) $(0.25, -600)$, (b) $(0.75, -600)$, (c) $(0.75, 100)$ and (d) $(0.25, 100)$, marked as red crosses on Fig. 3.b.